coefficient at the kth panel for the β mode, which is calculated from the doublet-lattice method using the following equation

$$\frac{\partial \bar{\phi}_\beta^k}{\partial x} + ik\bar{\phi}_\beta^k = \sum_s D_{ks}\Delta Cp_\beta^s(\omega) \tag{7}$$

where D_{ks} is the normal wash factor and k the reduced frequency. From Eqs. (2), (5), and (6), the power spectrum $S_{Q_\alpha}(\omega)$ is given as

$$\begin{aligned} S_{Q_\alpha}(\omega)\{1 - H_\alpha(\omega)E_{\alpha\alpha}(\omega) - H_\alpha^*(\omega)E_{\alpha\alpha}^*(\omega) \\ + |H_\alpha(\omega)|^2|E_{\alpha\alpha}(\omega)|^2\} \\ + |H_\alpha(\omega)|^2 \sum_{\substack{\beta \\ \beta\neq\alpha}} |E_{\beta\alpha}(\omega)|^2 S_{Q_\beta}(\omega) \\ = |H_\alpha(\omega)|^2 K_\alpha^2 S_{L_\alpha^D}(\omega) \end{aligned} \tag{8}$$

where

$$E_{\alpha\beta}(\omega) = K_\alpha \sum_k \bar{\phi}_\alpha^k \Delta Cp_\beta^k(\omega) A_k \tag{9}$$

Knowing $S_{Q_\alpha}(\omega)$, the acceleration spectra can be determined using Eq. (1) by differentiating with respect to time twice.

Example

As an example, the response of a F-4E wing is studied using structural and experimental wind tunnel rigid wing pressure fluctuation measurements given by Mullans and Lemley.[5] A total of 18 panels are used in the computations and the first 10 symmetric and antisymmetric bending modes are considered. Figure 2 shows a comparison between predictions and flight test data for the acceleration power spectral density measured at 84% semispan and 26% chord at $M=0.82$ and a dynamic pressure $Q=350$ psf. Two representations of the input random load power spectrum are used. The first assumes a constant correlation model where the pressure spectrum at any point in a panel and the pressure cross spectrum between two points in the same panel are both taken to be equal to the pressure spectrum at the panel center.[2] The second assumes an exponential spatially decaying form for the pressure cross spectrum using spearated flow decay coefficient data from Coe et al.[7] In all of the computations a value of 0.05 is used for the structural damping ratio. Using the constant correlation assumption, the comparisons with results from Ref. 5, which does not include the unsteady aerodynamic forces due to the wing vibration, show that unsteady air loads induced by the vibrating wing are quite important in the low-frequency range of the spectrum. However, at higher frequencies, they become less significant. Comparisons with flight test results show that the constant correlation assumption overestimates the response at the higher frequencies, but a great improvement in the predicitions is obtained by using the exponential spatially decaying form for the pressure cross-power spectrum. At low frequencies, due to inaccuracies in evaluating the decay coefficients obtained by extrapolating data[7] measured at much higher frequencies, it is found that predictions using the constant correlation assumption are in better agreement with flight test data than those obtained from the spatially decaying pressure cross-power spectrum representation.

Conclusions

A method for predicting the response of a wing to buffet loads has been presented. The unsteady aerodynamic forces generated by the vibrating wing are included in the analysis. It is shown that unsteady aerodynamic forces have a significant effect on the response predictions at low frequencies, while at higher frequencies they become less important.

In modeling the input load, the constant correlation assumption gives reasonable results at low frequencies, but at higher frequencies, the exponential spatially decaying form of the cross-power spectrum for the fluctuating pressures gives results which are in much better agreement with flight test data.

References

[1] Lee, B.H.K., "A Method for the Prediction of Wing Response to Non-Stationary Buffet Loads," National Research Council Canada, NRCC AR LR-601, July 1980.

[2] Schweiker, J.W. and Davis, R.E., "Response of Complex Shell Structures to Aerodynamic Noise," NASA CR-450, April 1966.

[3] Rodden, W.P., Giesing, J.P., and Kalman, T.P., "Refinement of the Nonplanar Subsonic Doublet-Lattice Lifting Surface Method," *Journal of Aircraft,* Vol. 9, Jan. 1972, pp. 69-73.

[4] Kalman, T.P., Rodden, W.P., and Giesing, J.P., "Application of the Doublet-Lattice Method to Nonplanar Configurations in Subsonic Flow," *Journal of Aircraft,* Vol. 8, June 1971, pp. 406-413.

[5] Mullans, R.E. and Lemley, C.E., "Buffet Dynamic Loads During Transonic Maneuvers," Air Force Flight Dynamics Laboratory, Tech. Rept. AFFDL-TR-72-46, Sept. 1972.

[6] Lee, B.H.K., "Aeroelastic Response of an Aircraft Wing to Random Loads," National Research Council Canada, NRCC AR LR-613, April 1983.

[7] Coe, C.F., Chyu, W.J., and Dods, J.B. Jr., "Pressure Fluctuations Underlying Attached and Separated Supersonic Turbulent Boundary Layers and Shock Waves," AIAA Paper 73-996, Oct. 1973.

Airfoil Probe for Angle-of-Attack Measurement

Paul J. Hermann*
Iowa State University, Ames, Iowa

Dennis B. Finley†
General Dynamics Corporation, Fort Worth, Texas

Steven C. Rehfeldt‡
McDonnell Douglas Astronautics Company, St. Louis, Missouri

and

Lowell C. Benishek§
McDonnell Douglas Technical Services Company, Houston, Texas

Introduction

CURRENT methods of sensing angle of attack[1] include use of vanes that line up with local flow, tapped hemispherical probes from which pressure differential measurements are obtained and translated into angle-of-attack and sideslip-angle information, and servo-driven null-

Received Feb. 4, 1983; revision received March 24, 1983.

*Associate Professor, Department of Aerospace Engineering. Associate Fellow AIAA.

†Aerodynamics Engineer, Aeroanalysis Group. Member AIAA.

‡Associate Engineer, Guidance and Control Department.

§Associate Engineer, Shuttle ASCENT/ABORT Flight Design Group.

seeking pressure tubes that are servo-aligned with the local flow to equalize differential pressures sensed from the probe. Several years ago the suggestion was made that a small, appropriately tapped airfoil might serve well as an angle-of-attack sensing probe.[2] Potential advantages of such a probe were perceived to be simplicity, since the probe would involve no moving parts external to the aircraft, and possible improvement in accuracy, since flow over an airfoil would be used rather than flow over a hemisphere or cylinder.

A feasibility study was conducted at Iowa State University to evaluate the potential of a small airfoil as an angle-of-attack sensing probe in low-speed low-dynamic pressure environments. A theoretical evaluation using techniques presented in Ref. 3 indicated that there should be significant variation with angle of attack of pressure coefficients on the surface of the airfoil, and that differential pressure coefficients for an airfoil should be increased by a factor of 2 or more in comparison with coefficients obtainable from flow over a hemisphere. Wind tunnel tests in a slow-speed wind tunnel on a small rectangular wing with NACA 0012 airfoil section demonstrated that significant differential pressure coefficients could be obtained. A laboratory system was developed and tested to demonstrate the feasibility of providing digital form and fed to an onboard computer for proessing to produce digital angle-of-attack and dynamic pressure data to an onboard digital flight control computer.

The Proposed System

A schematic diagram of the system proposed and evaluated in this study is shown in Fig. 1. The probe is to be a small canard wing mounted at some suitable location on the side of the fuselage, much as current angle-of-attack sensors are located. Pressure sensing taps are to be located on the upper and lower surfaces of the probe, probably in the forward 10% of the chord of the airfoil. Pressure leads transmit the pressures sensed at the taps to analog pressure differential transducers. The differential pressure measurements are converted to digital form and fed to an onboard computer for processing to produce digital angle-of-attack data to the flight control computer and/or a cockpit display.

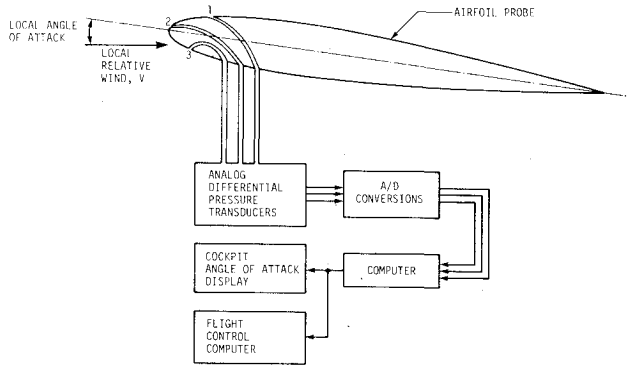

Fig. 1 Schematic diagram of angle-of-attack sensor and feedback system.

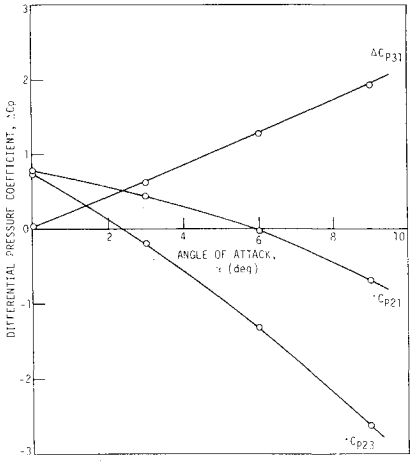

Fig. 2 Differential pressure coefficient calibration curves.

Static pressures sensed at the taps depend upon dynamic pressure and angle of attack. A theoretical study in which the relatively simple techniques of Ref. 3 were applied showed that one could expect maximum differentials between taps on the upper and lower surfaces at about 5% chord position. In addition, the theory indicates that the variation of differential pressure coefficient with angle of attack should be essentially linear. For this study, Reynolds and Mach number effects were ignored, since wind tunnel test section speeds used in experimental studies were less than 150 ft/s.

In principle, at least two independent sets of pressure differential measurements must be provided to the computer so that dynamic pressure information may be extracted, thereby permitting calculation of angle of attack. Thus a minimum of three pressure taps must be utilized. The technique proposed and used in this study was to calibrate two independent differential pressure coefficients from the probe as functions of angle of attack, and, to use these calibration functions in the computer to convert measured differential pressures into angle-of-attack information. Dynamic pressure may be determined as a byproduct of the computation.

Results

Wind tunnel testing was conducted in the Iowa State University slow-speed wind tunnel. The test article was a well-tapped half-wing mounted on a base on the floor of the test section. Airfoil section was an NACA 0012 airfoil. The wing had a chord, c, of 12.00 in. and a span of 17.69 in. from the base to the tip. Tip clearance from the top of the test section was about 0.7c. Pressure differential measurements for more than a dozen pairs of taps were made to determine the best pairs for further use in testing. The taps selected were as shown in Fig. 1. Tap 1 is on the upper surface at 7.5% chord. Tap 2 is on the upper surface just aft of the leading edge at 0.5% chord. Tap 3 is on the lower surface at 5% chord. Figure 2 shows typical calibration curves for the three sets of taps taken two at a time. The two pressure differentials used in testing of the proposed system were $\Delta P_{31} = P_3 - P_1$ and $\Delta P_{23} = P_2 - P_3$.

The calibration curves are shown to be slightly curvilinear. These curves were approximated by the following quadratic function

$$\Delta P = q(a\alpha^2 + b\alpha + c) \tag{1}$$

where q is dynamic pressure, and the coefficients for each pair of taps were determined from a least-squares fit to calibration data. Using Eq. (1) for each pair of pressure taps on the probe, it is possible to obtain the formula

$$\alpha = -\left[\frac{b_1 - \beta b_2}{2(a_1 - \beta a_2)}\right] + \sqrt{\left[\frac{b_1 - \beta b_2}{2(a_1 - \beta a_2)}\right]^2 - \left[\frac{c_1 - \beta c_2}{a_1 - \beta a_2}\right]} \tag{2}$$

where $\beta = \Delta P_{31}/\Delta P_{23}$, and the subscripts *1* and *2* refer to pressure differentials ΔP_{31} and ΔP_{23}, respectively.

A laboratory version of the system shown in Fig. 1 was developed and tested at four wind tunnel test section speeds between about 93 and 130 ft/s. The test probe angles of attack was set manually. Computed angles of attack from the pressure differential measurements were displayed on the screen of a computer. Computed values were compared with the manually set values. Results showed computed values to be within 0.1 deg of the manually set values over a range of angle of attack from -14.0 to $+6.0$ deg, and to be within 0.5 deg over a range from -16.0 to $+16.0$ deg.

There are two basic sources of error for the system. The first is in calculation of the differential pressure ratio $\beta = \Delta P_{31}/\Delta P_{23}$. This error can be produced by errors in the analog differential pressure transducers as well as by the A/D conversions in providing differential pressure data to the computer. The second source of error is in the accuracy by which the assumed quadratic calibration curves truly represent differential pressure coefficients as functions of angle of attack. Sensitivity of system output to the first of these errors was shown to be quite low at +2.0 deg in this study but to increase drastically as angle of attack increased. Sensitivity to the second of these errors was shown to be relatively small.

Conclusions

This study has shown that a small airfoil probe, consisting of a small canard wing mounted appropriately on an airframe and properly tapped, can serve as a viable alternative as a probe for angle-of-attack sensing on aircraft. An NACA 0012 airfoil section was used in wind tunnel tests in this study, and differential pressure coefficients greater than 3.0 at high angles of attack were achieved. These coefficients are an improvement by a factor of 2.0-3.0 over comparable coefficients obtained from hemispherical probes.

References

[1] Gracey, W., "Summary of Methods of Measuring Angle of Attack on Aircraft," NACA TN 4351, 1958.

[2] Hall, J., Collins Avionics and Missiles Group, Rockwell International, Cedar Rapids, Iowa, private communication, 1974.

[3] Kuethe, A. M. and Chow, C.-Y., "Properties of the Symmetrical Airfoil," *Foundations of Aerodynamics: Bases of Aerodynamic Design*, 3rd ed., John Wiley and Sons, New York, 1976, pp. 122-126.

Minimum Induced Drag of Wings with Curved Planform

J. Ashenberg* and D. Weihs†
Technion—Israel Institute of Technology, Haifa, Israel

Nomenclature

a = lift slope of wing section
A_n = nth coefficient of Fourier decomposition of spanwise distribution of circulation
$\mathcal{R}$ = aspect ratio
b = wing semispan
c = wing chord
f = lifting line shape function
K_I, K_T = defined by Eq. (3)
V = freestream velocity
W_I, W_T = self-induced and wake-induced downwash velocities, respectively.
x,y = coordinates in the streamwise and spanwise directions, respectively
α = angle of attack of wing cross section
Γ = sectional circulation on the wing divided by the freestream velocity and wing semispan
ϵ = coefficient of parabolic lifting line defined by $f = \epsilon y^2$
θ = trigonometric transform of spanwise coordinate, $\theta = -\cos^{-1} y$
ξ,η = dummy coordinates in x,y directions, respectively

Received May 16, 1983; revision received June 20, 1983.

*Graduate Student, Department of Aeronautical Engineering.
†Professor, Department of Aeronautical Engineering.

Introduction

ONE of the classical results of incompressible aerodynamics is that the minimum induced drag on a thin flat wing of given lift is obtained when the downwash is constant.[1] This results in the well-known elliptical distribution of chord length and vorticity for straight wings.

This result has since been generalized in various directions. Kuchemann[2] showed that minimal induced drag for swept wings is obtained for a planform wider at the root and narrower at the tips than the elliptical shape. Other workers analyzed cases of wings of given lift distribution,[3] root moment, and given structural weight[4] for swept, straight planforms.

In the present Note, the problem of minimizing induced drag for given lift in the case of wings with a curved center line (line of sectional centers of pressure), including both forward and backward sweep (see Fig. 1), is examined within the framework of lifting-line theory.

Analysis

The analysis is obtained for planforms of aspect ratio $\mathcal{R} \gg 1$, radius of curvature $0(\mathcal{R})$, and only slight $0(\mathcal{R}^{-1})$ deviations from planar wings. The derivation of this theory was described in detail in Ref. 5, so that only the relevant highlights are shown here.

Classical lifting-line theory is based on the assumption that $(x-\xi)^2 \ll (y-\eta)^2$ almost everywhere, as $\mathcal{R} \gg 1$. This leads to $\eta/\xi = 0(\mathcal{R})$ almost everywhere. This approach is generalized to curved wings by allowing $\xi = f(\eta) + 0(c)$ as the radius of curvature is large everywhere. The requirement of a finite radius of curvature leads to a self-induced component of downwash on the lifting line, which did not exist in straight lifting-line theory.[1-3] An integral equation[5] is obtained for the curved lifting line, correct to first order in $\mathcal{R}$

$$\int_{-b}^{b} \frac{d\Gamma}{d\eta} \frac{1}{y-\eta} \left(1 + \frac{x-f}{(x-f)^2 + (y-\eta)^2}\right) d\eta + \int_{-b}^{b} \Gamma(\eta) \frac{x - f' y + f' \eta - f}{[(x-f)^2 + (y-\eta)^2]^{3/2}} d\eta = -4\pi\alpha(y) \quad (1)$$

The second term on the left-hand side of Eq. (1) is the new term describing the self-induced velocity. This is a singular integral equation, but the singularity which is obtained for $y = \eta$ is removed by taking a finite core radius for the vortex. This well-known technique[7] results in a new unknown, the core radius. This is obtained by calculating the induced drag twice, once in the Trefftz plane far downstream, and independently on the wing. Both results are obtained as a function of the yet unknown core radius, so that equating them gives the core size. The spanwise distribution of circulation can be written in terms of a Fourier series

$$\Gamma(\theta) = 4 \sum_{n=1}^{\infty} A_n \sin(n\theta)$$

Equation (1) is then[5]

$$\sum_{n=1}^{\infty} \{8 \sin n\theta + a_\infty(\theta) c(\theta) [K_I(n,\theta) \cos\alpha + n K_T(n,\theta)]\} A_n = a(\theta) c(\theta) \alpha(\theta) \quad (2)$$

and

$$W_I = \sum_{n=1}^{\infty} A_n K_I(n,\theta) \quad \text{and} \quad W_T = \sum_{n=1}^{\infty} n A_n K_T(n,\theta) \quad (3)$$